MOLECULAR AND CELLULAR BIOLOGY, May 2008, p. 3177–3189 Vol. 28, No. 10
0270-7306/08/$08.00+0 doi:10.1128/MCB.01759-07

Redundant Roles of *Tead1* and *Tead2* in Notochord Development and the Regulation of Cell Proliferation and Survival[▽]

Atsushi Sawada,[1]† Hiroshi Kiyonari,[2] Kanako Ukita,[1] Noriyuki Nishioka,[1] Yu Imuta,[1] and Hiroshi Sasaki[1]*

Laboratory for Embryonic Induction[1] and Laboratory for Animal Resources and Genetic Engineering,[2] RIKEN Center for Developmental Biology, 2-2-3 Minatojima-minamimachi, Chuo-ku, Kobe, Hyogo 650-0047, Japan

Received 26 September 2007/Returned for modification 6 November 2007/Accepted 14 February 2008

Four members of the TEAD/TEF family of transcription factors are expressed widely in mouse embryos and adult tissues. Although in vitro studies have suggested various roles for TEAD proteins, their in vivo functions remain poorly understood. Here we examined the role of *Tead* genes by generating mouse mutants for *Tead1* and *Tead2*. *Tead2*$^{-/-}$ mice appeared normal, but *Tead1*$^{-/-}$; *Tead2*$^{-/-}$ embryos died at embryonic day 9.5 (E9.5) with severe growth defects and morphological abnormalities. At E8.5, *Tead1*$^{-/-}$; *Tead2*$^{-/-}$ embryos were already small and lacked characteristic structures such as a closed neural tube, a notochord, and somites. Despite these overt abnormalities, differentiation and patterning of the neural plate and endoderm were relatively normal. In contrast, the paraxial mesoderm and lateral plate mesoderm were displaced laterally, and a differentiated notochord was not maintained. These abnormalities and defects in yolk sac vasculature organization resemble those of mutants for *Yap*, which encodes a coactivator of TEAD proteins. Moreover, we demonstrated genetic interactions between *Tead1* and *Tead2* and *Yap*. Finally, *Tead1*$^{-/-}$; *Tead2*$^{-/-}$ embryos showed reduced cell proliferation and increased apoptosis. These results suggest that *Tead1* and *Tead2* are functionally redundant, use YAP as a major coactivator, and support notochord maintenance as well as cell proliferation and survival in mouse development.

The TEAD proteins comprise a conserved family of eukaryotic DNA-binding proteins (27, 30). The first member discovered, TEAD1 (also known as transcriptional enhancer factor 1), was originally cloned in human cells as an activator of the simian virus 40 enhancer (12, 65). The TEAD family transcription factors contain an evolutionarily conserved DNA-binding domain called the TEA domain, which forms a three-helix bundle with a homeodomain fold (2). There are four closely related *Tead* genes (*Tead1* to *Tead4*) (26, 27, 30) in mice and humans. *Tead* gene family members are also found in invertebrates, including *Drosophila* and *Caenorhabditis elegans* (22, 53, 63, 71), and less conserved orthologs are found in the fungi *Saccharomyces cerevisiae*, *Aspergillus nidulans*, and *Candida albicans* (3, 18, 50). Genetic studies in invertebrates have revealed various biological roles for the *Tead* genes. The *Drosophila Tead* gene *Scalloped (Sd)* is required for wing development (22, 53), and the product of the *C. elegans Tead* gene, *egl-44*, suppresses the differentiation of touch-sensitive cells while promoting the differentiation of the motor neurons responsible for egg laying (63, 71). In contrast to these well-characterized functions in invertebrates, the roles of the *Tead* genes in vertebrates remain unclear.

In mammals, the four *Tead* genes are expressed widely, but with distinct patterns, from preimplantation embryos to adult tissues (27, 29, 30, 70). Most adult tissues express at least one *Tead* gene, and some tissues, such as lung, abundantly express all four of them. The developmental stage- and tissue-specific expression of the four *Tead* genes suggests that each one may play a distinct role. Consistent with the global expression patterns of the *Tead* genes, in vitro studies and in vivo transgenic approaches have suggested that the TEAD proteins regulate a wide range of developmental processes, including skeletal and cardiac muscle development, skeletal muscle regeneration, neural crest development, and notochord development (19, 20, 32, 41, 49). However, these roles have not been clearly supported by genetic analyses involving *Tead* gene inactivation in the mouse. In a *Tead1* mutant mouse generated by gene-trapping in embryonic stem (ES) cells, the *Tead1* homozygous mutant embryos died at embryonic day 11.5 (E11.5) with heart defects (11). Although the results from many in vitro experiments suggest that TEAD regulates cardiac muscle-specific genes, the differentiation of cardiac muscle was not compromised in the *Tead1* mutants; rather, the cardiac muscle growth was severely affected. Likewise, a heterozygous missense mutation of human *TEAD1* was recently identified as a causative allele for helicoid peripapillary chorioretinal degeneration (16). In addition, recent analyses of *Tead4* mutant mice showed that *Tead4* is essential for trophectoderm specification but is dispensable for postimplantation development (44, 67). However, such roles for *Tead1* and *Tead4* had not been suggested by previous in vitro analyses. One possible explanation for such discrepancies is that functional redundancy among the *Tead* genes compensates for the absence or reduction of *Tead* in most tissues and masks the roles suggested by in vitro studies. Alternatively, each *Tead* gene may have distinct roles that have not been revealed by in vitro studies.

* Corresponding author. Mailing address: Laboratory for Embryonic Induction, RIKEN Center for Developmental Biology, 2-2-3 Minatojima-minamimachi, Chuo-ku, Kobe, Hyogo 650-0047, Japan. Phone: (81) 78 306 0102. Fax: (81) 78 306 3363. E-mail: sasaki@cdb.riken.jp.

† Present address: Department of Biological Sciences, Vanderbilt University, Nashville, TN 37235.

▽ Published ahead of print on 10 March 2008.

The transcriptional activator function of the TEAD proteins appears to require their interaction with coactivator proteins (22, 53, 65). Although in vitro studies have identified several candidates for coactivators of mammalian TEAD proteins, the contribution of these coactivator proteins to TEAD activity in vivo is not known. In *Drosophila*, the TEAD protein Sd uses Vestigial (Vg) as a coactivator protein (22, 53). While *Sd* is expressed in various imaginal discs, *Vg* expression is restricted to the wing imaginal disc. *Sd* and *Vg* act as selector genes whose products, Sd and Vg, form an active complex only in the wing disc, and this complex regulates wing development (21). Although the ectopic expression of Vg in other imaginal discs promotes ectopic wing development (33), a similar selector role for Sd in other imaginal discs has not been found (17, 54). Therefore, although Sd is expressed widely, it exerts a selector function only in the wing disc. Since Sd function can be replaced by human TEAD1, the activity of mammalian TEAD proteins might be regulated in a similar way. In support of this notion, mice and humans have four *Vg* homologues (*Vgll1* to *Vgll4*), and human Vgll1 (also known as TONDU) can compensate for Vg function in *Drosophila* wing development (10, 59). Mouse *Vgll2* is specifically expressed in skeletal muscle and may play a role in muscle differentiation (9, 37).

While the Sd-Vg complex operates only in wing development, experiments using a recessive lethal allele of *Sd* or the inhibition of Sd's activator function show Sd to be a transcriptional activator in leg, eye, and optic lobe development (17, 54). Therefore, Sd must use other unidentified transcriptional coactivators in these tissues. In mammals, in vitro studies identified YAP1 (Yes-associated protein 1 [also known as YAP65], hereafter referred to as YAP) as a coactivator of TEAD proteins (58). YAP is an adaptor protein containing multiple protein interaction domains and an acidic transcriptional activation domain similar to that found in the herpes simplex virus protein VP16 (66). Under in vitro conditions, YAP has a much stronger coactivator activity than Vglls (37, 58). A YAP-related protein, Wwtr1 (also known as TAZ), shows a comparable coactivator activity for TEAD proteins (39). Both of these candidate TEAD coactivators have been inactivated in the mouse. In contrast to the heart-restricted defects observed with the *Tead1* mutant mouse, *Yap* mutant mice show gross abnormalities that include small body size, shortened body axis, and defects in yolk sac vasculogenesis and chorioallantoic fusion (42). *Wwtr1* mutant mice survive to term but die postnatally of glomerulocystic kidney disease (24). Therefore, the contribution of these factors to the transcriptional activity of TEAD proteins in mouse development remains unclear.

In this study, to investigate the roles of the mammalian TEADs in vivo, we generated mouse mutants for the *Tead1* and *Tead2* genes. *Tead2*$^{-/-}$ mutants appeared normal, but *Tead1*$^{-/-}$; *Tead2*$^{-/-}$ double mutant embryos showed general growth retardation and severe morphological abnormalities by E8.5, indicating that *Tead1* and *Tead2* have redundant functions in development. The *Tead1*$^{-/-}$; *Tead2*$^{-/-}$ embryos showed defects in mesoderm development, especially in the notochord. Furthermore, phenotypic similarities between the *Tead1*$^{-/-}$; *Tead2*$^{-/-}$ and *Yap*$^{tm1/tm1}$ mutant embryos as well as genetic interactions between *Tead1* and *Tead2* and *Yap* suggest that YAP is a major coactivator protein of TEAD1 and TEAD2 in vivo.

MATERIALS AND METHODS

Mouse strains. *Tead1* and *Tead2* mutant mice (accession numbers CDB0410K and CDB0404K, respectively) were generated as follows. The C57BL/6 mouse bacterial artificial chromosome genomic DNA clones RPCI24-359I13 and RPCI24-372P9, which contain the translation initiation sites of the *Tead1* and *Tead2* genes, respectively, were obtained from BACPAC Resources, Children's Hospital Oakland Research Institute, and were used for the isolation of genomic DNA fragments. To construct the targeting vectors, we first generated MC1-DT-A-pA/pMW118 by cloning a cassette consisting of the MC1 promoter, diphtheria toxin A (DT-A) gene fragment, and the poly(A) signal of the *Pgk* gene (34) into the KpnI-HindIII sites of a low-copy-number plasmid, pMW118 (Nippon Gene, Japan). The *Tead1* targeting vector was constructed by cloning a 15-kb Eco47III-SalI fragment containing the second exon of the *Tead1* gene into MC1-DT-A-pA/pMW118, followed by the replacement of an internal NaeI-AgeI fragment containing the second exon with a *Pgk* gene promoter-*neo*-poly(A) signal cassette flanked by *loxP* sites and a splice acceptor (SA) signal of En2-IRES-β-geo-poly(A) (SA-IRES-β-geo-pA, where IRES is internal ribosome entry site) cassette. The *Tead2* targeting vector was similarly constructed by replacing the second and third exons with SA-IRES-β-geo-pA between a 6.5-kb AflIII-NruI fragment containing the first exon and a 6-kb AflIII-AflIII fragment containing the fourth exon. TT-2 ES cells (68) were electroporated with linearized targeting vectors, followed by positive and negative selection with G418 and DT-A, respectively. ES clones were first screened for homologous recombination by long PCR using LA-*Taq* (TaKaRa, Japan), as described previously (43). For the screening of *Tead1* and *Tead2* loci, the primer pair Tead1 S2 (5′-CGATGCCT GCTTGCCGAATATCATG-3′) and Tead1 R4 (5′-GGCTCCACAAGTCATG TGAAGTC-3) and the pair Tead2 S5 (5′-CTTCCTCGTGCTTTACGGTATC-3′) and Tead2 R10 (5′-CAAGGTTTGCAATGGCTAAGCAG-3′), respectively, were used. The positions of these primers are indicated in Fig. 1A. Homologous recombination of the *Tead* loci was confirmed for clones that were positive by PCR and by Southern hybridization of the ES genome with 5′ and 3′ external genomic probes, and the absence of random targeting-vector insertion was also confirmed with an internal probe for the *lacZ* gene that detects β-*geo*. The resultant ES clones were injected into 8-cell-stage embryos to produce chimeric mice. Chimeric founders from two independent ES cell lines were crossed with C57BL/6 mice, and the resulting mutant mouse lines were maintained on either an inbred C57BL/6 or outbred CD1 (Charles River) background. The mutant phenotypes were not affected by ES cell line origin or genetic background.

For genetic interaction studies, *Tead1*$^{+/-}$; *Tead2*$^{+/-}$ mice were crossed with *Yap*$^{+/tm1Smil}$ (hereafter referred to as *Yap*$^{+/tm1}$) mice (38), which were kindly provided by E. Morin-Kensicki and S. L. Milgram. Mice were housed in environmentally controlled rooms of the Laboratory Animal Housing Facility of the RIKEN Center for Developmental Biology, under the institutional guidelines for animal and recombinant DNA experiments.

Genotype determination by PCR. The genotypes of adults and embryos were identified by PCR of DNAs prepared from ear punches and yolk sacs, respectively. A mixture of the following three primers was used: for examination of the *Tead1* locus: Tead1-F1 (5′-CAGCCATATCACATCTGTAGAGG-3′), Tead1-F2 (5′-CTTTCTGTGGCACTGAGCCTCTCAG-3′), and Tead1-R2 (5′-ACTCTCCTTCTGCCTTAGACTCCTG-3′); for the *Tead2* locus, Tead2-S2 (5′-CGATGCCTGCTTGCCGATATCATG-3′), Tead2-F2 (5′-ACATAGCTAGA ACACGGCTGAGCTG-3′), and Tead2-R2 (5′-GAGCACTTAGCACCAAGC CTAGTTC-3′). The locations of the primers are indicated in Fig. 1A. The PCR conditions were as follows: 94°C for 3 min and 30 cycles of 94°C for 30 s, 59°C for 30 s, and 72°C for 1 min 30 s, followed by 72°C for 5 min. Genotype determination of the *Yap*^{tm1} allele was also performed by PCR under conditions described previously (38).

Reverse transcription-PCR (RT-PCR). The total RNAs were prepared from E8.5 wild-type and *Tead1*$^{-/-}$; *Tead2*$^{-/-}$ mutant embryos using an RNeasy Mini kit (Qiagen) and were used in a reverse transcription reaction with Ready-to-Go You-Prime First-Strand Beads (Amersham Biosciences) according to the manufacturer's instructions. The resulting cDNA pools were used for PCR amplification of the *Tead1*, *Tead2*, and β-*actin* cDNA fragments. The primers for each gene were as follows: Tead1-1, 5′-TACTGCCATCCACAACAAGC-3′ and 5′-TGCTGCACAAAGGGCTTGAC-3′; Tead1-2, 5′-CTCCGCTTTCCTTGAAC AGC-3′ and 5′-GTCCACAGATTCGAGCAACG-3′; Tead2-1, 5′-CCTGATGC AGAAGGTGTGTG-3′ and5′-ACCTGAATATGGCTGGAGAC-3′; Tead2-2, 5′-GAGAAATTCAGTCCAAGCTG-3′ and 5′-TCTGGAACATTCCATGGT GG-3′; Tead2-3, 5′-GCCACCATGGAATGTTCCAG-3′ and 5′-GAGAACTC TGTCAGCTGCAG-3′; Tead2-4, 5′-TGAGCAGCCAGTATGAGAGC-3′ and 5′-CAGCAGACGGTACACAAAGC-3′; and β-actin, 5′-TGTATGCCTCTGG TCGTACCACAG-3′ and 5′-GATGTCACGCACGATTTCCCTCTC-3′.

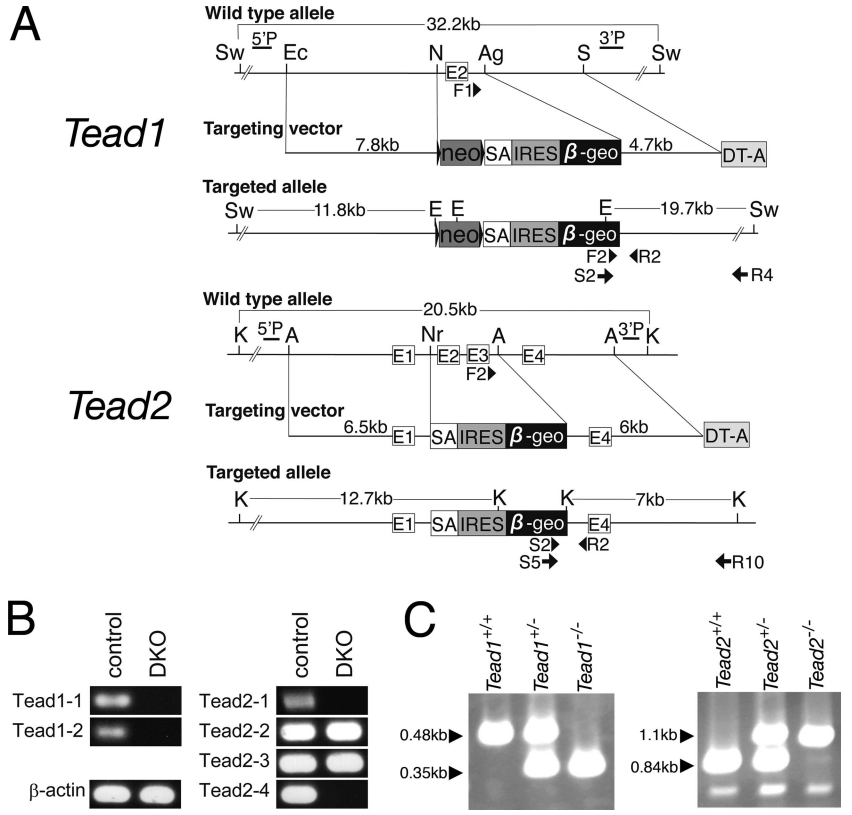

FIG. 1. Targeted disruption of the *Tead1* and *Tead2* genes. (A) The *Tead1* mutant allele was generated by replacing exon 2, containing the translation initiation site, with the *loxP-Pgk-neo*-poly(A)-*loxP* cassette (neo) and the SA-IRES-β-geo-pA signal cassette. The *Tead2* mutant allele was generated by replacing exons 2 and 3, containing the translation initiation site and half of the TEA domain, with SA-IRES-β-geo-pA. See Materials and Methods for details. Positions of the 5′ and 3′ probes for Southern hybridization are indicated as 5′P and 3′P, respectively. Positions of the PCR primers used for the initial screening of homologous recombinants and genotype identifications are indicated by arrows and arrowheads, respectively. Abbreviations are as follows: Sw, SwaI; Ec, Eco47III; N, NaeI; Ag, AgeI; S, SalI; E, EagI; K, KpnI; A, AflIII; Nr, NruI; DT-A, MC1-DT-A-pA cassette. (B) Expression of *Tead1* and *Tead2* transcripts in the mutant embryos. RT-PCR was performed using RNAs isolated from E8.5 control or $Tead1^{-/-}$; $Tead2^{-/-}$ (DKO) embryos and primer sets for various regions of *Tead1* and *Tead2* cDNAs. In the double mutant embryos, no *Tead1* transcript was detected. Although some transcripts were detected for *Tead2* (Tead2-2 and Tead2-3), these transcripts lacked coding regions for the TEA domain and coactivator-interacting domain (Tead2-1 and Tead2-4). These truncated *Tead2* transcripts would not encode a functional protein. (C) Genotype determination by PCR. The genotypes of the embryos were clearly identified by PCR amplification of yolk sac genomic DNA fragments with a mixture of the three primers indicated by arrowheads in panel A (*Tead1* locus: F1, F2, and R2; *Tead2* locus: F2, S2, and R2).

The primers for Tead1-2, Tead2-4, and β-actin were originally described in Nishioka et al. (44). The PCR conditions were as follows: 94°C for 3 min and 30 cycles of 94°C for 30 s, 57°C for 30 s, and 72°C for 1 min 30 s, followed by 72°C for 10 min.

In situ hybridization. Mouse embryos were staged by morphology (14). In situ hybridization was performed according to standard procedures (47, 61) with the following modifications. The sodium dodecyl sulfate in the hybridization buffer was replaced by 3-[(3-cholamidopropyl)dimethylammonio]-1-propanesulfonate (CHAPS), and the antibody reaction was performed in maleic acid buffer (100 mM maleic acid, 150 mM NaCl [pH 7.5]) instead of phosphate-buffered saline. The following probes were used to detect specific genes: *Sox2* (a gift from R. Lovell-Badge); *Otx2* (40); *Krox20* (51); *Hoxb1* (a gift from H. Koseki); *Hoxb9* (a gift from K.-I. Yamamura); *Afp* and *Brachyury* (gifts from A. Shimono); *Foxa1*, *Foxa2*, and *Foxc1* (47); *Sox17* (28); *Meox1* (6); *Noto* (1); α-*globin* (7); and *Yap* (49).

Analysis of cell proliferation and apoptosis. Mitotic cells were detected by a standard immunohistochemical procedure using an anti-phospho-histone H3 rabbit polyclonal antibody (1:100 dilution) (Upstate) as the primary antibody. Apoptotic cells were detected by terminal deoxynucleotidyltransferase-mediated dUTP-biotin nick end labeling (TUNEL) using an Apoptosis Detection Kit (Chemicon) according to the manufacturer's instructions. Nuclei were detected by light counterstaining with hematoxylin. The numbers of total and phospho-H3- or TUNEL-positive cells were counted for two or three sections, respectively, per embryo. Mitotic and apoptotic indices were analyzed with Prism5 statistical software (GraphPad) using an unpaired, one-tailed *t* test and applying Welch's correction when appropriate.

RESULTS

Generation of $Tead1^{-/-}$ and $Tead2^{-/-}$ mutant mice. We previously identified the TEAD family transcription factors as key regulators of the *Foxa2* enhancer in the node and notochord (49). However, the in vitro and transgenic approaches we used did not reveal the roles of individual *Tead* genes in *Foxa2* expression or in embryonic development. Therefore, to clarify the roles of individual *Tead* genes, we generated *Tead* mutant mice. Because the expression level of *Tead2* during embryogenesis is much higher than that of the other *Tead* genes (29, 49), we first focused on the *Tead2* gene. We disrupted *Tead2* by replacing the second and third exons, which contain the translation start site and half of the TEA DNA-binding domain, with a cassette consisting of a SA-IRES-β-

geo-pA signal (Fig. 1A). In mice homozygous for this allele, we detected no *Tead2* transcripts containing the deleted exons by RT-PCR with probe Tead2-1, which amplified exons 2 to 4 (Fig. 1B). Unexpectedly, however, we did detect *Tead2* transcripts by RT-PCR using probes amplifying some downstream exons (Tead2-2, exons 4 to 6; Tead2-3, exons 6 to 8), but transcripts of the exons further downstream (Tead2-4, exons 10 to 11) were not detected (Fig. 1B). Therefore, any protein produced from the truncated *Tead2* transcripts would lack part of the DNA-binding and coactivator-interaction domains and should be nonfunctional; therefore, the *Tead2* mutant allele should be a null allele. The genotypes of the embryos were routinely identified by PCR of the yolk sac DNAs (Fig. 1C). *Tead2*$^{-/-}$ mice exhibited no overt abnormalities and were fertile, indicating that *Tead2* is dispensable for development and growth (data not shown).

We hypothesized that *Tead2* and the other *Tead* genes are functionally redundant and, therefore, that other *Tead* genes compensated for the absence of *Tead2*. Thus, to reveal a potentially masked *Tead2* function, we generated compound mutants of *Tead1* and *Tead2*. We selected *Tead1* because a homozygous gene trap mutation of *Tead1* is embryonic lethal around E11.5 (9) and because *Tead1* and *Tead2* show widespread overlapping expression between E7.5 and E9.0, except in the heart, where only *Tead1* is expressed (49). Therefore, if *Tead1* and *Tead2* had any redundant functions in early development, a further reduction of the *Tead* gene dosages would exacerbate the mutant phenotype. To generate the *Tead1* mutant mouse, the *Tead1* gene was disrupted by replacing the second exon, which contains the translation initiation codon, with the PGK-*neo*-pA cassette and the SA-IRES-β-geo cassette described above (Fig. 1A). The *Tead1*$^{-/-}$ mutant mice died around E11.5. The major defect was a reduction of myocardium trabeculation (data not shown), as previously reported for the gene-trap mutant (9). Some of our mutants died even earlier, perhaps because of the difference in the genetic backgrounds of the mutant mice (data not shown). We confirmed the proper homologous recombination of the *Tead* loci and the absence of randomly inserted targeting vectors in the mutant ES cells by Southern hybridization (data not shown). We also confirmed the absence of *Tead1* transcripts by RT-PCR analyses using primer sets that amplify two regions of the downstream exons (Tead1-1, exons 7 to 9; Tead1-2, exons 10 to 11) in embryos that were homozygous mutants for this allele (Fig. 1B) and genotyped the embryos by PCR using yolk sac DNA (Fig. 1C).

To generate the *Tead1*$^{-/-}$; *Tead2*$^{-/-}$ double mutant mice, we first generated *Tead1*$^{+/-}$; *Tead2*$^{+/-}$ mice by crossing *Tead1*$^{+/-}$ animals and *Tead2*$^{-/-}$ animals. Since both the *Tead1* and *Tead2* genes are on the same chromosome (Chr7), the resulting *Tead1*$^{+/-}$; *Tead2*$^{+/-}$ mice should have the targeting alleles on separate chromosomes (*trans*-heterozygous). The *Tead1*$^{+/-}$; *Tead2*$^{+/-}$ mice did not exhibit any obvious abnormalities. To obtain *cis*-heterozygous animals, which have both targeted alleles on the same chromosome following a meiotic crossover event, the *trans*-heterozygous mice were crossed to wild-type mice. Of the progeny obtained with this cross, 14.6% were *Tead1*$^{+/-}$; *Tead2*$^{+/-}$ *cis*-heterozygotes. We then intercrossed the *cis*-heterozygous *Tead1*$^{+/-}$; *Tead2*$^{+/-}$ animals to obtain *Tead1*$^{-/-}$; *Tead2*$^{-/-}$ double homozygous mutant mice. As anticipated from the observed *Tead1*$^{-/-}$ embryonic lethality, we failed to obtain *Tead1*$^{-/-}$; *Tead2*$^{+/+}$, *Tead1*$^{-/-}$; *Tead2*$^{+/-}$, or *Tead1*$^{-/-}$; *Tead2*$^{-/-}$ mice at weaning. Notably, we also did not identify any *Tead1*$^{+/-}$; *Tead2*$^{-/-}$ mice at the weaning age, suggesting that this genotype is either embryonic lethal or early postembryonic lethal. Approximately half of the *Tead1*$^{+/-}$; *Tead2*$^{-/-}$ embryos showed an anterior neural tube closure defect or exencephaly between E9.5 and E15.5 (see Fig. 8C and D and data not shown). Morphologically abnormal *Tead1*$^{-/-}$; *Tead2*$^{-/-}$ embryos were consistently found at E9.5 but were not recovered after E12.5 (data not shown). To elucidate the events leading to the severe morphological abnormalities of the *Tead1*$^{-/-}$; *Tead2*$^{-/-}$ mutant embryos, we next examined the abnormalities of the double homozygous mutant embryos in detail.

***Tead1*$^{-/-}$; *Tead2*$^{-/-}$ embryos showed severe morphological defects at E8.5.** At E6.5, the *Tead1*$^{-/-}$; *Tead2*$^{-/-}$ embryos were morphologically indistinguishable from sibling control embryos (data not shown). At E7.5, the mutant embryos were slightly smaller than their siblings but appeared normal histologically (Fig. 2A and B and data not shown). At E8.5, however, the mutant embryos were small and showed dorso-ventral undulations (Fig. 2C and D). Histological examination of the mutants showed that the anterior region was dorsally folded and there were two heart tubes, indicating that the two heart primordia failed to fuse (Fig. 2F). In the central region, in contrast to the wild-type embryos, the mutant neural plate had not fused along the dorsal ridges to form a neural tube. Instead, the neural plate remained flat, and the boundary between the neuroectoderm and the underlying mesoderm was not clearly demarcated (Fig. 2G). In the posterior region of the embryos, the boundary between the neuroectoderm and presomitic mesoderm was clearer (Fig. 2H). The notochord and somites were morphologically indistinct throughout the length of the body. At E8.75, the mutants failed to undergo embryonic turning, their neural plate was kinked dorso-ventrally, and an abnormal protrusion to the ventral side developed at the posterior end of the mutant embryo (Fig. 2J and K). In this region, abnormal cell accumulation was observed (Fig. 2K). At E9.5, the mutant embryos were much smaller than the control embryos and were highly disorganized morphologically (see Fig. 8A, B, and H). They typically developed a characteristic posterior-ventral protrusion and a bulbous allantois that failed to fuse with the chorion (see Fig. 8H).

Specification and anteroposterior patterning of the neuroectoderm were relatively normal in *Tead1*$^{-/-}$; *Tead2*$^{-/-}$ embryos. To dissect the abnormalities observed in the *Tead1*$^{-/-}$; *Tead2*$^{-/-}$ embryos, we examined the expression of various molecular markers at E8.5. In all these experiments, we examined the expression of each marker gene in more than three mutant embryos and found consistent results unless noted. We first examined development of the neuroectoderm. At this stage in control embryos, the entire neural plate/tube expressed *Sox2*. In the *Tead1*$^{-/-}$; *Tead2*$^{-/-}$ embryos, *Sox2* expression was observed along the entire body axis, indicating that specification of the neuroectoderm occurred normally (Fig. 3A and B). To examine the anteroposterior patterning of the neural plate, we next analyzed the expression of the following regionally restricted genes: *Otx2* (forebrain and midbrain) (52), *Krox20* (third rhombomere [r3] and r5) (51),

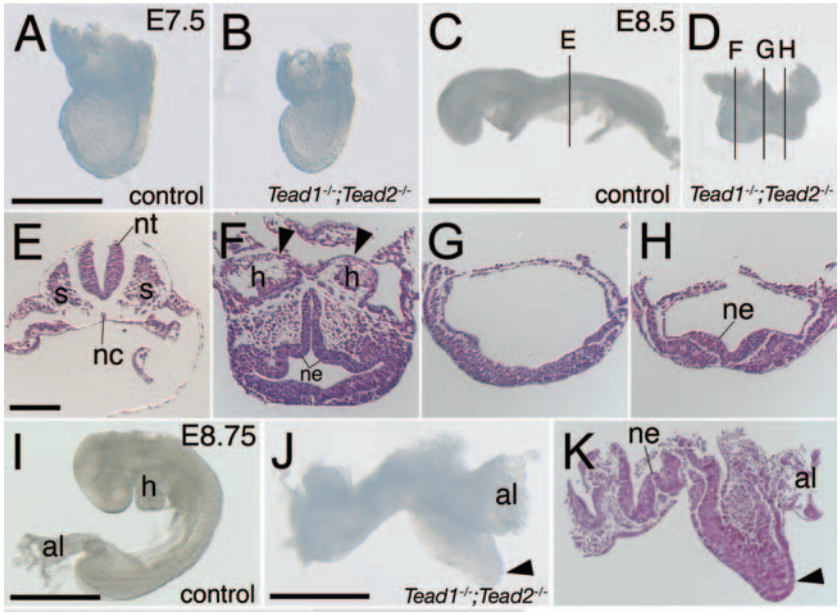

FIG. 2. Gross phenotypes of the *Tead1*$^{-/-}$; *Tead2*$^{-/-}$ mutant embryos. External views (A to D, I, and J) and histological sections (F to H and K) of control (A, C, E, and I) and *Tead1*$^{-/-}$; *Tead2*$^{-/-}$ (B, D, F to H, J, and K) embryos. Anterior is to the left. Images shown in panels E and F to H are transverse sections of the images shown in panels C and D, respectively. The approximate positions of sections are indicated in panels C and D. Panel K shows a sagittal section of panel J. The *Tead1*$^{-/-}$; *Tead2*$^{-/-}$ embryos were smaller than control embryos. Although the mutants were morphologically normal at E7.5 (B), their morphology was disorganized by E8.5 (D). Heart tubes failed to fuse (arrowheads in panel F). At E8.75, the neural plate undulated dorsoventrally, and an abnormal protrusion developed in the posterior-ventral region (arrowheads in panels J and K). Abbreviations: h, heart tubes; nc, notochord; ne, neuroectoderm; nt, neural tube; s, somite; al, allantois. Scale bars and use of the same scalfe in other panels are as follows: 400 μm (A; also panel B), 1 mm (C; also panel D), 100 μm (E; also panels F to H), 1 mm (I), and 500 μm (J; also panel K).

Hoxb1 (r4 and posterior to the thoracic level) (62), and *Hoxb9* (posterior to the thoracic level) (5). In mutant embryos, all of these markers were expressed in the proper regionally restricted manner in the same anteroposterior order as in the control embryos (Fig. 3C to J). These results suggested that, irrespective of the gross morphological abnormalities, specification of the neural plate and its patterning along the anteroposterior axis took place relatively normally in the *Tead1*$^{-/-}$; *Tead2*$^{-/-}$ embryos.

Endoderm development in the *Tead1*$^{-/-}$; *Tead2*$^{-/-}$ embryo was relatively normal except for the posterior definitive endoderm. We next examined endoderm development in the *Tead1*$^{-/-}$; *Tead2*$^{-/-}$ embryos. At this stage, the endoderm is divided into two types, the visceral endoderm and the definitive endoderm. In normal development, the visceral endoderm, which transiently covers the embryonic region of the embryo, is displaced by the definitive endoderm and forms the visceral yolk sac by associating with the extraembryonic mesoderm. Visceral endoderm development was characterized by examining the expression of *Alpha-fetoprotein* (*Afp*) at E8.5 (15) (Fig. 4A). In mutant embryos, *Afp* expression was clearly observed in the extraembryonic area, suggesting that the visceral endoderm was developing normally (Fig. 4B). As a marker of definitive endoderm development, we used *Foxa1*, which is normally expressed widely in the definitive endoderm except for the posterior region surrounding the node and primitive streak (Fig. 4C) (47). This expression pattern was maintained in the *Tead1*$^{-/-}$; *Tead2*$^{-/-}$ embryos, although the boundary between the *Foxa1*-positive and -negative regions was more evident in the mutants (Fig. 4D). Supporting the idea of normal endoderm development in the mutant, Foxa2 protein expression was observed in all the endoderm cells of the mutant embryos, as in the controls (data not shown) (47). In contrast, the expression of *Sox17* in the definitive endoderm, which was normally restricted to the posterior region, was clearly downregulated in the mutants (n = 3/4) (Fig. 4E and F) (28). Interestingly, the expression of *Sox17* was increased (n = 3/4) in the mutant mesoderm-derived allantois, which was expanded laterally (Fig. 4F). These results suggest that development of the visceral and definitive endoderm were relatively normal in the *Tead1*$^{-/-}$; *Tead2*$^{-/-}$ embryos, although development of the posterior definitive endoderm was partially compromised.

Paraxial mesoderm and lateral plate mesoderm were displaced toward the lateral margins in *Tead1*$^{-/-}$; *Tead2*$^{-/-}$ embryos. Histologically, the development of the paraxial mesoderm appeared most severely affected in the *Tead1*$^{-/-}$; *Tead2*$^{-/-}$ embryos. No morphologically identifiable somites were formed, and in the central portion of the body, no paraxial mesoderm could be recognized on the ventral side of the neural plate (Fig. 2F to H). Therefore, we first examined the development of the paraxial mesoderm, which is characterized by the expression of *Foxc1* (formerly known as *MF1*) (47). *Foxc1* is also expressed in the head mesenchyme. *Foxc1* expression in the *Tead1*$^{-/-}$; *Tead2*$^{-/-}$ embryos was almost normal at E7.5 (Fig. 5A to D), but *Foxc1*-positive cells were displaced laterally as development proceeded, and it became localized to the position corresponding to the lateral plate or the extraem-

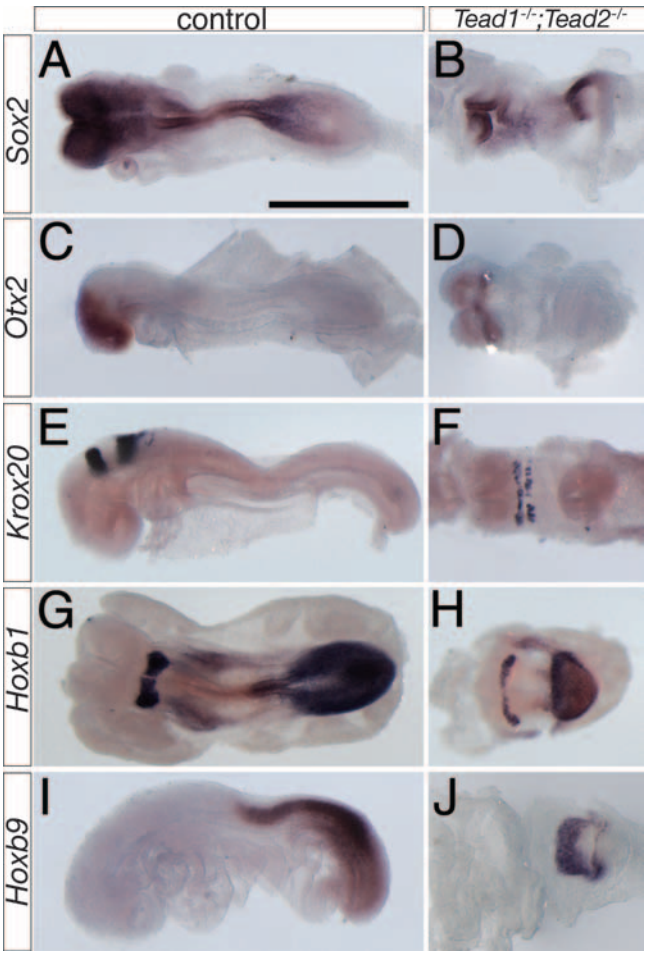

FIG. 3. Specification and anteroposterior patterning of the neuroectoderm were relatively normal in *Tead1*$^{-/-}$; *Tead2*$^{-/-}$ embryos. Control and *Tead1*$^{-/-}$; *Tead2*$^{-/-}$ embryos were examined for expression of the pan-neural gene *Sox2* (A and B) and regionally restricted genes *Otx2* (C and D, fore- and midbrain), *Krox20* (E and F, r3 and r5), *Hoxb1* (G and H, r4 and posterior to the thoracic region) and *Hoxb9* (I and J; posterior to the thoracic region). In spite of the gross morphological abnormalities, the mutant embryos retained an essentially proper spatial organization of gene expression patterns. Scale bar, 1 mm (same scale used for all panels).

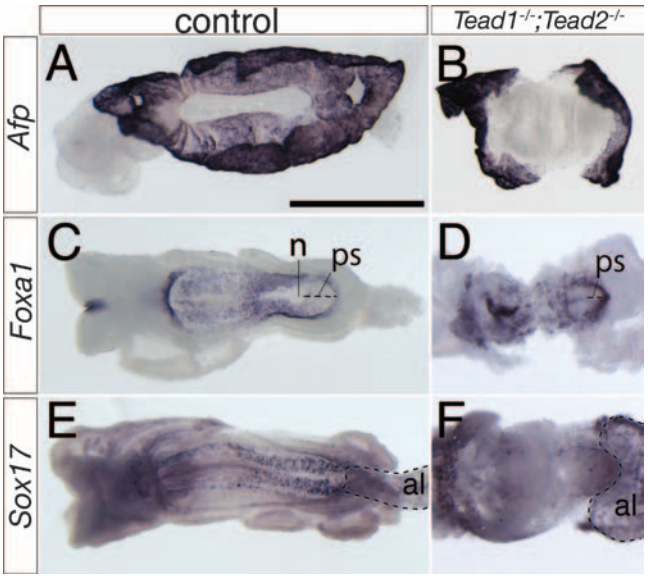

FIG. 4. Endoderm development in the *Tead1*$^{-/-}$; *Tead2*$^{-/-}$ embryo was relatively normal except for the posterior definitive endoderm. Control and *Tead1*$^{-/-}$; *Tead2*$^{-/-}$ embryos were examined for the expression of a visceral endoderm-specific gene, *Afp* (A and B) and definitive endoderm genes, *Foxa1* (C and D) and *Sox17* (E and F). Specification of the visceral and definitive endoderm occurred relatively normally except for the posterior definitive endoderm region, in which the expression of *Sox17* was reduced. Abbreviations: al, allantois; n, node; ps, primitive streak. Scale bar, 1 mm (same scale used for all panels).

bryonic mesoderm of normal embryos after E8.0 (Fig. 5E to G and data not shown). *Foxc1* expression at the posterior end of the embryos retained a more medial position up to E8.75 (Fig. 5F and J) Although the segmented somites were not morphologically identifiable, the expression of *Meox1* (formerly known as *Mox1*), which is specific to the somites (6) (Fig. 5I), was also observed in laterally displaced domains (Fig. 5K and data not shown). Interestingly, despite the absence of morphologically segmented somites, the expression of *Foxc1* and *Meox1* in the posterior region of the mutant embryos sometimes formed weak stripes (Fig. 5F, G, and K). The lateral plate mesoderm revealed by *Foxf1* expression (38) was also displaced to the lateral margins in the mutants (data not shown). Taken together, these results suggest that, in terms of cell differentiation, development of the paraxial mesoderm (including head mesenchyme and somites) and lateral plate mesoderm occurred normally in the mutants, but they were displaced toward the lateral margins.

The notochord was not maintained in *Tead1*$^{-/-}$; *Tead2*$^{-/-}$ embryos. We previously identified TEAD family proteins as key regulators of the *Foxa2* enhancer, which drives the expression of *Foxa2* in the node and the notochord (49). Between E6.5 and E8.25, *Foxa2* is expressed in the axial tissues, which include the gastrula organizer, the node, the notochord, and the presumptive floor plate of the neural tube/plate (47); and we observed similar expression in the *Tead1*$^{-/-}$; *Tead2*$^{-/-}$ embryos (Fig. 6A and B and data not shown). However, by E8.5, *Foxa2* expression in the mutant became discontinuous (Fig. 6C), and it disappeared except at the anterior tip of the embryo by E8.75 (Fig. 6D). The anterior expression domain may correspond to the prechordal plate and/or the ventral midline of the anterior-most neural plate.

As anticipated by the essential role of *Foxa2* in node and notochord development (4, 60), *Brachyury* expression in the node and notochord (23) of the mutant embryos was normal at E8.25 but became discontinuous by E8.5 (Fig. 6F and G). At E8.75, *Brachyury* expression in the notochord was lost or nearly absent (n = 9/9), as was its expression in the node/posterior end of the notochord (n = 6/9), although this expression in some embryos was not significantly affected (n = 3/9) (Fig. 6H and data not shown). Defects in the notochordal development were further evidenced by a discontinuous and reduced expression of *Noto*, which is normally restricted to the posterior notochord (1), at E8.5 (data not shown). *Brachyury* expression in the primitive streak was maintained, indicating that the

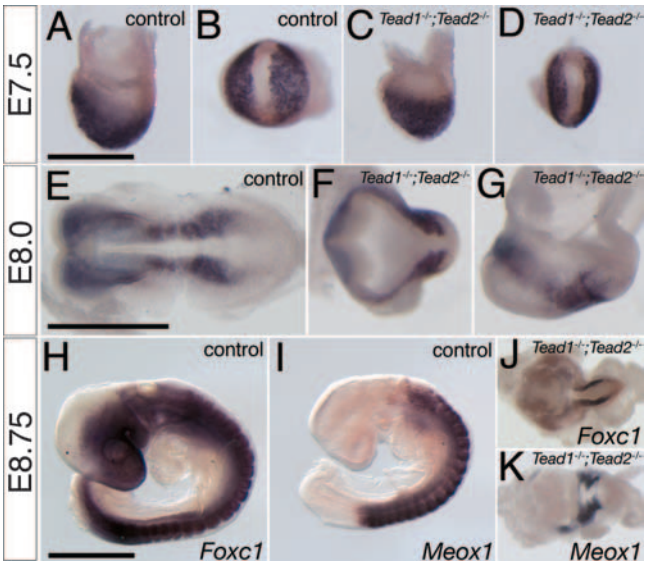

FIG. 5. Paraxial mesoderm was physically displaced toward the lateral margins in *Tead1*$^{-/-}$; *Tead2*$^{-/-}$ embryos. Control and *Tead1*$^{-/-}$; *Tead2*$^{-/-}$ embryos were examined for expression of a paraxial mesoderm gene, *Foxc1* (A to H and J) and a somite-specific gene, *Meox1* (I and K). The *Foxc1* expression domain was normal at E7.5, but it was displaced toward the lateral edges at E8.0 and E8.75. *Foxc1* was also expressed in the anterior region of the mutants, but that expression domain is obscured by other tissue in panel J. Similar lateral expression was also observed for *Meox1* at E8.75. Panels A, C, G, H, and I show lateral views; panels B, D, F, J, and K show ventral views; panel E shows a dorsal view. Scale bars and use of the same scale in other panels are as follows: 400 μm (A; also panels B to D), 750 μm (E; also panels F and G), and in 800 μm (H; also panels I to K).

development of specifically the axial mesoderm was disturbed (Fig. 6G and H). That the development of the primitive streak was normal was further supported by its relatively normal expression of *Fgf8*, *Wnt3a*, and *Tbx6* (8, 56, 69) in the *Tead1*$^{-/-}$; *Tead2*$^{-/-}$ embryos (data not shown). Taken together, although the *Tead1*$^{-/-}$; *Tead2*$^{-/-}$ embryos were clearly morphologically abnormal, major cell types in these embryos formed and were patterned in a relatively normal manner. In contrast, notochord development was clearly defective.

***Tead1*$^{-/-}$; *Tead2*$^{-/-}$ embryos showed extraembryonic defects similar to those of *Yap* mutant mice.** Previous in vitro studies identified the YAP protein as a coactivator of TEAD family transcriptional factors (58). A *Yap*$^{tm1Smil/tm1\ Smil}$ (hereafter referred to as *Yap*$^{tm/tm1}$) mutant mouse was recently reported by Morin-Kensicki et al., and the abnormalities observed in the *Yap* mutant embryos resemble those of the *Tead1*$^{-/-}$; *Tead2*$^{-/-}$ mutants (42). Because *Yap*$^{tm1/tm1}$ mutant embryos have defects in yolk sac vasculogenesis, we next examined whether the *Tead1*$^{-/-}$; *Tead2*$^{-/-}$ mutants exhibited similar extraembryonic defects. Staining with an antibody to platelet endothelial cell adhesion molecule 1 (PECAM-1), which marks endothelial cells, revealed that endothelial cells differentiated but failed to organize into vessels (Fig. 7A and B). In addition, expression of the α-*globin* gene indicated the existence of erythroblasts in the disorganized yolk sac of the *Tead1*$^{-/-}$; *Tead2*$^{-/-}$ embryos (Fig. 7C and D). Therefore, in the mutant yolk sac, specification of both components of the early yolk sac vasculature (endothelia and erythroblasts) occurred, but their development into an organized primitive vascular plexus was compromised. These features of the *Tead1*$^{-/-}$; *Tead2*$^{-/-}$ yolk sac resembled those of the *Yap*$^{tm1/tm1}$ embryo. However, these phenotypic similarities were not caused by the reduced expression of *Yap* in *Tead1*$^{-/-}$; *Tead2*$^{-/-}$ mutants because the *Yap* expression level in the *Tead1*$^{-/-}$; *Tead2*$^{-/-}$ embryos was comparable to that in control embryos, as revealed by whole-mount in situ hybridization (Fig. 7E and F). Taken together, the similarities in both the embryonic and yolk sac phenotypes of the *Tead1*$^{-/-}$; *Tead2*$^{-/-}$ and *Yap*$^{tm1/tm1}$ mutant embryos support the hypothesis that the TEAD1 and TEAD2 proteins use YAP as a coactivator protein in exerting their transcriptional activator function during embryogenesis.

***Tead1* and *Tead2* genetically interacted with *Yap*.** If TEAD1/TEAD2 functions by forming a complex with YAP during development, the simultaneous reduction of TEAD1/TEAD2 and YAP should reduce the amount of this complex and cause similar developmental defects as observed with the *Tead1* and *Tead2* compound mutants. Therefore, we generated the compound mutants of *Tead1*; *Tead2*; *Yap* and compared their phenotypes with those of the *Tead1*; *Tead2* mutants at E9.5. Because we obtained *Tead1*$^{+/-}$; *Tead2*$^{+/-}$; *Yap*$^{+/tm1}$ male mice that showed no obvious abnormalities, we crossed these mice to *Tead1*$^{+/-}$; *Tead2*$^{+/-}$ females to obtain the compound mutant embryos. Approximately half of the *Tead1*$^{+/-}$; *Tead2*$^{-/-}$

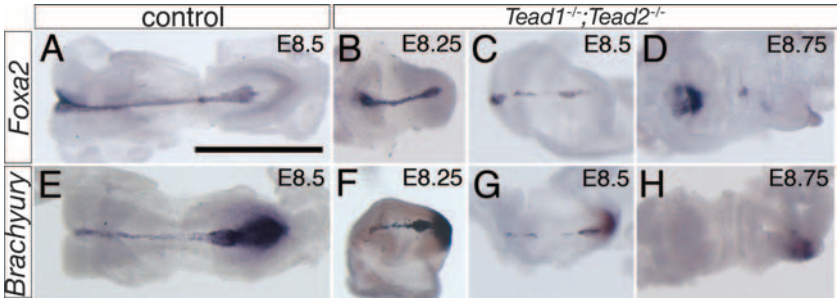

FIG. 6. Axial mesoderm formed but was not maintained in *Tead1*$^{-/-}$; *Tead2*$^{-/-}$ embryos. Expression of *Foxa2* and *Brachyury* was examined in control and mutant embryos. Anterior is to the left. *Foxa2* expression was detected in the midline tissue, including the prechordal plate, the floor plate of the neural tube/plate, the notochord, and the node (A). In the mutant embryos, *Foxa2* expression was initially normal at E8.25 (B) but became discontinuous by E8.5 (C) and was lost except for the anterior tip at E8.75 (F). Similar changes in *Brachyury* expression in the node and notochord were observed (F to H). Scale bar, 1 mm (same scale used for all panels).

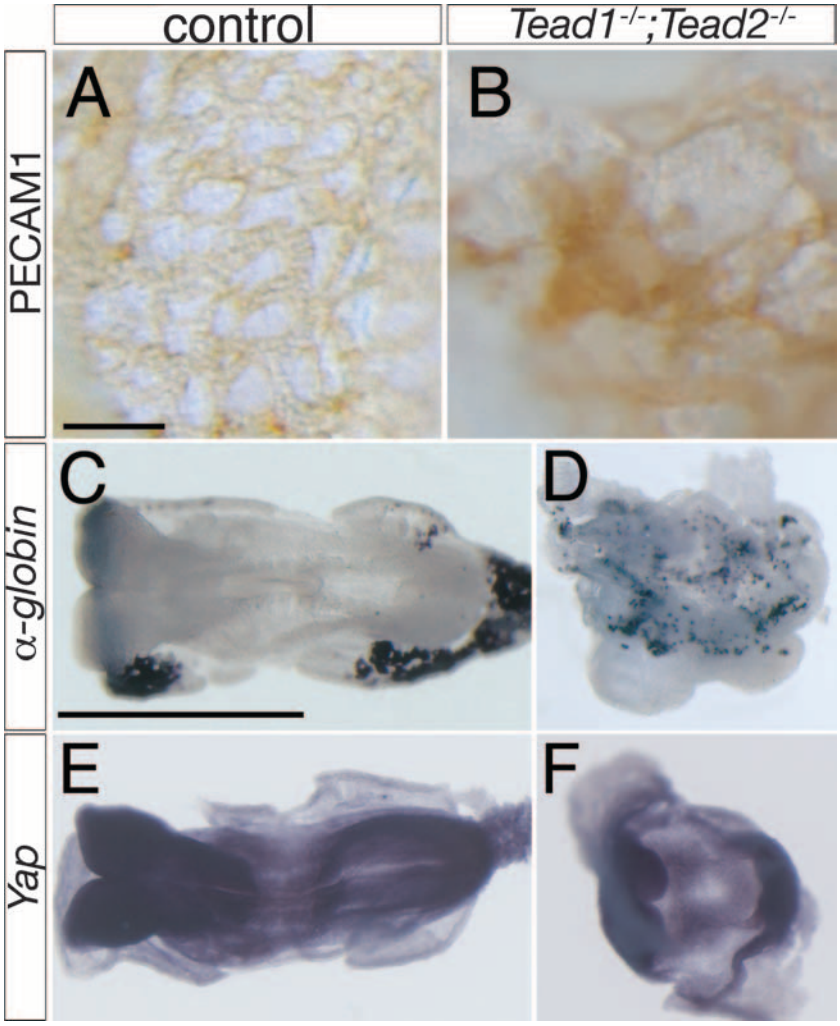

FIG. 7. Vascular organization in the yolk sac was disorganized in *Tead1*$^{-/-}$; *Tead2*$^{-/-}$ embryos. Expression of PECAM-1, α-*globin*, and *Yap* was examined in control (A, C, and E) and mutant (B, D, and F) embryos. PECAM-1-positive endothelial cells were differentiated in the mutant yolk sac, but they failed to form organized vasculature (B). Erythroblasts expressing α-*globin* also formed in the mutant yolk sac (D). Although the *Tead1*$^{-/-}$; *Tead2*$^{-/-}$ embryos resembled *Yap*$^{tm1/tm1}$ mutants, *Yap* expression in the *Tead1*$^{-/-}$; *Tead2*$^{-/-}$ embryos was not significantly affected (E and F). Scale bars, 100 μm (A; same scale used in panel B) and 1 mm (C; same scale used in panels D to F).

embryos (n = 3/6) showed anterior neuropore closure defects (Fig. 8A to D). The introduction of a heterozygous mutation of *Yap* in this genetic context (*Tead1*$^{+/-}$; *Tead2*$^{-/-}$; *Yap*$^{+/tm1}$) caused additional abnormalities including smaller posterior tissues and defective embryonic turning (n = 2/2) (Fig. 8E). The *Tead1*$^{-/-}$; *Tead2*$^{+/-}$ embryos were clearly developmentally delayed but resembled normal E8.5 embryos (n = 8/8) (Fig. 8F). The introduction of a heterozygous mutation of *Yap* in this genetic context (*Tead1*$^{-/-}$; *Tead2*$^{+/-}$; *Yap*$^{+/tm1}$) resulted in severe morphological defects that were essentially the same as those of the *Tead1*$^{-/-}$; *Tead2*$^{-/-}$ embryos (n = 3/4) (Fig. 8G). Embryos with both of these genotypes developed a posterior-ventral protrusion and a bulbous allantois (Fig. 8G and H). Introduction of the heterozygous *Yap* mutation to the *Tead1*$^{-/-}$; *Tead2*$^{-/-}$ mutants (*Tead1*$^{-/-}$; *Tead2*$^{-/-}$; *Yap*$^{+/tm1}$) did not significantly alter the phenotype (n = 7/7) (Fig. 8I). These results clearly demonstrated a genetic interaction between *Tead1* and *Tead2* and *Yap*.

Foxa2 expression in the notochord is directly regulated by TEAD proteins (49), and its expression was down-regulated in the *Tead1*$^{-/-}$; *Tead2*$^{-/-}$ embryos (Fig. 6). Therefore, if TEAD1/TEAD2 uses YAP as a major coactivator, the *Yap*$^{tm1/tm1}$ embryos should also show reduced *Foxa2* expression. Indeed, as anticipated by the discontinuous *Brachyury* expression in the notochord of *Yap*$^{tm1/tm1}$ embryos at E9.5 (42), the *Foxa2* expression in the *Yap*$^{tm1/tm1}$ embryos between E8.75 and E9.5 was either strongly down-regulated except for the anterior tip (n = 2/7) (Fig. 8J) or discontinuous and gradually down-regulated in the posterior region (n = 5/7) (Fig. 8K). Taken together, the genetic interactions as well as the similarities of the mutant phenotypes support the hypothesis that YAP is the major coactivator protein of TEAD1 and TEAD2 in mouse embryogenesis.

Cell proliferation decreased, and the incidence of apoptosis increased in *Tead1*$^{-/-}$; *Tead2*$^{-/-}$ embryos. *Yap* was recently shown to have oncogenic activities (45, 72). Moreover, consis-

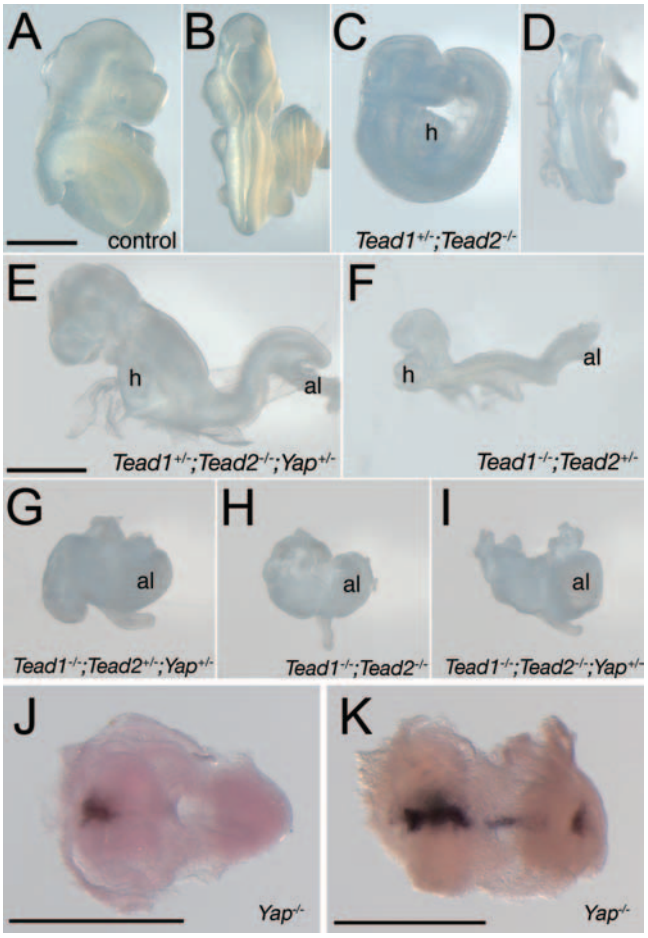

FIG. 8. *Tead1* and *Tead2* genetically interacted with *Yap*. (A to I) External morphologies of wild-type and *Tead1*; *Tead2*; *Yap* compound mutant embryos at E9.5. Half of the $Tead1^{+/-}$; $Tead2^{-/-}$ embryos showed an open-brain phenotype (C and D), and the $Tead1^{+/-}$; $Tead2^{-/-}$; $Yap^{+/tm1}$ embryos showed additional defects in posterior development and embryonic turning (E). The $Tead1^{-/-}$; $Tead2^{+/-}$ embryos showed severe growth retardation (F), and $Tead1^{-/-}$; $Tead2^{+/-}$; $Yap^{+/tm1}$ embryos showed severe morphological abnormalities (G), which resembled those of $Tead1^{-/-}$; $Tead2^{-/-}$ embryos (H). The $Tead1^{-/-}$; $Tead2^{-/-}$; $Yap^{+/tm1}$ embryos (I) were essentially the same as $Tead1^{-/-}$; $Tead2^{-/-}$ embryos. The $Tead1^{-/-}$; $Tead2^{+/-}$; $Yap^{+/tm1}$, $Tead1^{-/-}$; $Tead2^{-/-}$ and $Tead1^{-/-}$; $Tead2^{-/-}$; $Yap^{+/tm1}$ embryos all developed a characteristic protrusion at the posterior-ventral region (arrowheads in panels G, H, and I) and had a bulbous allantois. (J and K) *Foxa2* expression in $Yap^{tm1/tm1}$ mutant embryos. Expression of the TEAD1/TEAD2 target gene, *Foxa2*, was either strongly down-regulated except for the anterior tip (J) or discontinuous and gradually down-regulated at the posterior region (K) in the $Yap^{tm1/tm1}$ embryos. Embryos shown in J and K are at E8.75 and E9.5, respectively. Abbreviations: h, heart; al, allantois. Scale bars, 1 mm (A and E; same scale used for panels A to I) and 600 nm (J and K).

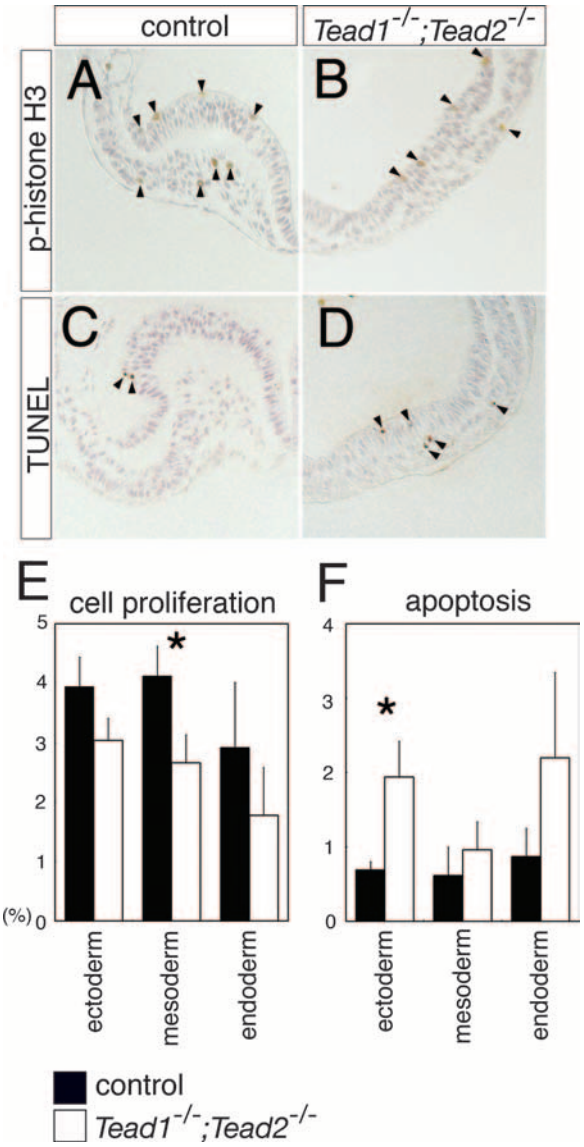

FIG. 9. Cell proliferation and apoptosis were altered in $Tead1^{-/-}$; $Tead2^{-/-}$ embryos. (A to D) Sections showing the distribution of proliferating (A and B) and apoptotic (C and D) cells (arrowheads) in the control and $Tead1^{-/-}$; $Tead2^{-/-}$ embryos at E7.75. (E and F) Quantification of proliferating and apoptotic cells of control and $Tead1^{-/-}$; $Tead2^{-/-}$ embryos detected by anti-phospho-histone H3 and TUNEL labeling, respectively. Values shown represent the means and standard errors ($n = 5$) of the percentages of total cells that were positive. Black and white bars represent control and $Tead1^{-/-}$; $Tead2^{-/-}$ embryos, respectively. Asterisks above the bars indicate that the differences were statistically significant ($P < 0.05$).

tent with a role in growth regulation, $Yap^{tm1/tm1}$ embryos are smaller than sibling embryos by E9.5 (42). Because of the phenotypic similarities of the $Tead1^{-/-}$; $Tead2^{-/-}$ and $Yap^{tm1/tm1}$ embryos (42) and because of the genetic interaction between *Tead1* and *Tead2* and *Yap*, we speculated that *Tead* genes are also involved in growth regulation. Because the growth retardation of later-stage mutant embryos could be secondarily caused by insufficient circulation owing to the defects in the heart and yolk sac, we analyzed embryos at E7.75 (early to late head-fold stage) when embryonic growth does not yet depend on circulation and when the abnormalities of the mutant embryos are not yet morphologically evident.

To learn if *Tead1* and *Tead2* play a direct role in embryonic growth, we examined the frequency of both mitotic and apoptotic cells in the mutant embryos. We found that the frequency of mitotic cells detected by anti-phosphorylated histone H3 was significantly reduced in the $Tead1^{-/-}$; $Tead2^{-/-}$ mutants

(Fig. 9A, B, and E) (4.0% to 2.8%, $n = 5$) with a tendency to decrease in all the germ layers; the difference reached significance in the mesoderm. In addition, TUNEL labeling revealed an increased frequency of apoptotic cells in the mutants (Fig. 7C, D, and F) (0.66% to 1.7%, $n = 5$). The tendency toward increased apoptosis was observed in all the germ layers and reached significance in the ectoderm. These results suggest that *Tead1* and *Tead2* directly promote cell proliferation and survival.

DISCUSSION

In the present study, we examined the role of *Tead* genes in mouse embryogenesis by generating *Tead1* and *Tead2* mutant mice. *Tead1*$^{-/-}$; *Tead2*$^{-/-}$ embryos showed severe defects, including abnormalities in mesoderm patterning, notochord development, and embryonic growth. Neither *Tead1*$^{-/-}$ nor *Tead2*$^{-/-}$ embryos showed such morphological defects, indicating that *Tead1* and *Tead2* are functionally redundant in these processes. The similarity of the mutant phenotypes of *Tead1*$^{-/-}$; *Tead2*$^{-/-}$ and *Yap*$^{tm1/tm1}$ as well as the genetic interaction between *Tead1* and *Tead2* and *Yap* suggests that YAP is the major coactivator of the TEAD1 and TEAD2 proteins. Our analysis provides a clue to understanding the roles of *Tead* family genes during mouse development and their underlying mechanisms.

***Tead1* and *Tead2* are functionally redundant.** Mice and humans have four *Tead* genes, the encoded proteins of which are highly homologous, especially in their TEA domain (DNA-binding domain) and C-terminal coactivator-binding domain (26, 30). Because they have similar activities in vitro and their expressions widely overlap during embryogenesis (26, 49, 58), it is likely that the *Tead* genes play redundant roles in embryogenesis. However, this possibility has not been investigated. By generating mouse mutants for the *Tead1* and *Tead2* genes, we have demonstrated here that *Tead2*$^{-/-}$ mutant mice are apparently normal while *Tead1*$^{-/-}$; *Tead2*$^{-/-}$ double mutants show severe and widespread defects. This result clearly indicates that the roles of *Tead1* and *Tead2* in mouse embryogenesis largely overlap. Although we failed to detect clear abnormalities in the *Tead2*$^{-/-}$ embryos between E9.5 to 15.5 (data not shown), Kaneko et al. observed an exencephaly phenotype in a minor population of their *Tead2*$^{-/-}$ embryos (31). Because both Kaneko's group and our group deleted exons 2 and 3 to disrupt the *Tead2* locus, the reasons for the phenotypic differences are currently unknown. However, it is interesting that approximately half of the *Tead1*$^{+/-}$; *Tead2*$^{-/-}$ embryos also showed exencephaly. This similarity in mutant phenotypes between *Tead2*$^{-/-}$ and *Tead1*$^{+/-}$; *Tead2*$^{-/-}$ embryos also supports the notion that *Tead1* and *Tead2* play overlapping roles. Because *Tead2* is not expressed in the embryonic heart (26, 49), the heart-specific defects of the *Tead1*$^{-/-}$ mutants are likely to be attributable to the absence of a functionally redundant *Tead2* gene in the heart, rather than to a distinct function of *Tead1* in the heart. In support of this hypothesis, the heart defect observed in the *Tead1*$^{-/-}$ mutant (11) was a defect in the proliferation of myocardium (H. Sato and H. Sasaki, unpublished data), and defective cell proliferation was a characteristic feature of the *Tead1*$^{-/-}$; *Tead2*$^{-/-}$ double mutants. Therefore, *Tead1* and *Tead2* appear to play essentially the same roles in embryogenesis. In further support of the functional redundancy among *Tead* genes, *Tead4* is dispensable for ES cell differentiation and postimplantation development (44, 67), and *Tead3*$^{-/-}$ mice are apparently normal and fertile (A. S. and H. Sasaki, unpublished data). From these observations, we propose that the mammalian TEAD proteins have essentially the same activities in postimplantation development, with their functional differences being attributable to differences in their expression domains.

***Tead1* and *Tead2* are required for maintenance of notochord development.** In spite of the gross morphological abnormalities of *Tead1*$^{-/-}$; *Tead2*$^{-/-}$ mutant embryos at E8.5, the differentiation and patterning of the neuroectoderm and endoderm were relatively normal, while stark abnormalities were observed in the mesoderm. Although cell differentiation occurred, the relative positions of the paraxial mesoderm and lateral plate mesoderm were displaced toward the lateral margins. The underlying mechanism of this phenotype is not known, but a disturbance of the growth coordination between adjacent germ layers may explain such morphological defects. The *Tead1*$^{-/-}$; *Tead2*$^{-/-}$ embryos showed a reduction in cell proliferation that was more evident in the mesoderm than in the overlying ectoderm. Because mouse embryos develop in an inside-out manner continuous with the balloon-like yolk sac up to E8.5, it is likely that the rapidly expanding ectodermal sheet in the mutant could not be kept inside the more slowly growing sheets of paraxial and lateral plate mesoderm. As a consequence, the ectodermal sheet may have protruded by penetrating through the gap between the bilaterally located mesodermal sheets, physically displacing them to more lateral positions.

Only the notochord showed a clear developmental defect in the *Tead1*$^{-/-}$; *Tead2*$^{-/-}$ embryos. This result is consistent with our previous finding that TEAD proteins are key transcriptional regulators of the *Foxa2* enhancer (49). Because Foxa2 is a transcription factor essential for the development of the notochord and the node (4, 60), *Tead* genes should be required for node/notochord development. In *Tead1*$^{-/-}$; *Tead2*$^{-/-}$ embryos, the node and notochord formed initially, but they were not maintained after E8.5. Therefore, of the four TEAD proteins, TEAD1 and TEAD2 appear to be the major regulators of the *Foxa2* enhancer after E8.5. The activation of the *Foxa2* enhancer at earlier stages might be controlled by other TEAD proteins either exclusively or redundantly with TEAD1 and TEAD2. Alternatively, the earlier expression of *Foxa2* could be redundantly regulated by an unidentified enhancer that is independent of *Tead*. Supporting the latter possibility, only some of the enhancers have been identified for *Foxa2*, and the enhancer controlling its earlier expression in the gastrula organizer remains to be identified (48). Nevertheless, the abnormal development of the notochord clearly indicates the involvement of *Tead1* and *Tead2* in this process, and this function of the TEAD proteins is supported by both in vitro and in vivo genetic evidence (49).

YAP is a major coactivator protein of TEAD1 and TEAD2. In *Drosophila*, the TEAD protein Sd uses Vg as a coactivator protein (22, 53). Mice and humans each have four *Vg* homologues (*Vgll1-Vgll4*), and their involvement in skeletal muscle development as TEAD coactivator proteins has been suggested (10, 37, 59). On the other hand, biochemical studies in

mammals identified YAP and its related protein, Wwtr1, as TEAD coactivator proteins (39, 58). However, the major coactivator(s) of the TEAD proteins in vivo is not known. We show here that *Tead1*$^{-/-}$; *Tead2*$^{-/-}$ embryos were small at E8.5 and, despite relatively normal antero-posterior patterning, developed a discontinuous notochord and defective yolk sac vasculogenesis. All of these features are in common with the phenotype observed in *Yap*$^{tm1/tm1}$ mutant embryos (42). Furthermore, we also showed that *Tead1* and *Tead2* genetically interacted with *Yap* during embryogenesis and that a TEAD target gene, *Foxa2*, was down-regulated in *Yap*$^{tm1/tm1}$ mutant embryos. Although the *Yap*-related gene *Wwtr1* is also expressed at this stage (42), *Wwtr1*$^{-/-}$ mutants develop to term and show glomerulocystic kidney disease postnatally (24). Furthermore, *Vgll1*$^{-/-}$, *Vgll3*$^{-/-}$, and *Vgl1l*$^{-/-}$; *Vgll3*$^{-/-}$ mutant mice exhibited no overt abnormalities (H. Sato and H. Sasaki, unpublished data). The similarity of the mutant phenotypes and the genetic interactions strongly support the hypothesis that YAP is the major coactivator protein of TEAD1 and TEAD2 during early embryogenesis. Likewise, these results indicate that YAP functions primarily with TEAD proteins in early development. Although this does not rule out the possible involvement of Wwtr1 or Vgll proteins in the transcriptional activities of other TEAD proteins or of any TEAD proteins at different developmental stages, it is plausible that YAP is a major coactivator protein of all four TEAD proteins throughout development. This hypothesis can be genetically tested in the future by generating mice carrying mutations for the other *Tead* genes and by testing genetic interactions among the mutants of *Tead* and other potential coactivators.

***Tead1* and *Tead2* regulate cell proliferation and survival.** A striking feature of the *Tead1*$^{-/-}$; *Tead2*$^{-/-}$ embryos is their small size. Although growth defects could be secondarily caused by insufficient nutrition from circulation defects, our analysis at E7.75, which precedes heart formation, revealed that *Tead1* and *Tead2* directly regulate cell proliferation and survival. Although the impact of the deletion of *Tead1* and *Tead2* on proliferation and apoptosis was most evident in the mesoderm and ectoderm, respectively, the reason for such variation among germ layers is currently unknown. In further support of the idea that cell proliferation is controlled by TEAD proteins, we also observed significantly reduced bromodeoxyuridine labeling specifically in the myocardium of E9.5 *Tead1*$^{-/-}$ embryos (H. Sato and H. Sasaki, unpublished data). Recently, *Yap* was identified as an amplified gene in mammary tumors and liver cancers, and it was shown to have transforming properties, including the acceleration of proliferation and suppression of apoptosis (45, 72). Because our study strongly suggests that YAP is a major coactivator protein of TEAD1 and TEAD2, such growth-promoting activities of *Yap* may well be mediated by the transcriptional activities of TEAD1, TEAD2, and/or other TEAD proteins. Although *Yap* also has proapoptotic activity, this activity is mediated by p73 (55). Therefore, it is likely that the anti- and proapoptotic functions of *Yap* are mediated by distinct transcription factors, TEAD and p73, respectively.

The growth-regulatory activities of *Yap* appear to be evolutionarily conserved because overexpression of the *Drosophila Yap* homologue *Yki* also causes increased proliferation and reduced cell death (25). In *Drosophila*, Yki activity is negatively regulated by the Hippo (Hpo) signaling pathway, in which the Hpo-Sav complex activates the Wts kinase-Mats complex, which in turn inactivates Yki (reviewed in reference 46). The Hpo signaling pathway is likely to be conserved in mammals because (i) mammalian homologues exist for all the components; (ii) the human homologues of Hpo, Wts, and Mats can rescue their corresponding *Drosophila* mutants (35, 57, 64); and (iii) some of the components have tumor-suppressive activities in mammalian cells (36). In fact, a recent study demonstrated that Hpo-Yap signaling also regulates organ size in mouse (13). However, the transcription factor that acts downstream of Yap/Yki is currently unknown. Consistent with the essential role in cell survival played by *Drosophila* Sd (17), an intriguing hypothesis is that TEAD/Sd is one of the downstream effectors of the Hpo signaling pathway in regulating cell proliferation and survival.

Conclusion. Our genetic analyses of the roles of *Tead1* and *Tead2* indicate that these two TEAD proteins have largely redundant functions in mouse development. The major roles of *Tead1* and *Tead2* appear to be the promotion of cell proliferation and suppression of cell death, but *Tead1* and *Tead2* also clearly regulate development of the notochord. The similar mutant phenotypes and evidence of genetic interactions suggest that TEAD1/TEAD2 uses YAP as a major coactivator protein. Whether these features can be generalized to all the TEAD proteins or are specific to TEAD1/TEAD2 awaits the results of ongoing genetic analyses of the requirements for the *Yap* and *Tead* genes.

ACKNOWLEDGMENTS

We are grateful to the Laboratory for Animal Resources and Genetic Engineering for plasmids, the generation of mutant mice, and the housing of mice. We also thank E. M. Morin-Kensicki for critically reading the manuscript, E. M. Morin-Kensicki and S. L. Milgram for kindly providing the *Yap*^{tm1} mutant mice, M. Takahashi for a lecture on human *TEAD1* mutation, and A. Gossler, Y. Hayashizaki, B. Hermann, Y. Higashi, A. Joyner, Y. Kanai, H. Koseki, R. Lovell-Badge, G. Martin, I. Matsuo, R. Nusse, Y. Saga, A. Shimono, S. Takada, D. Wilkinson, C. Wright, and K.-I. Yamamura, for in situ hybridization probes.

This work was supported by a grant from the Japan Society for the Promotion of Science (JSPS) to A.S. (16770175) and grants from RIKEN, the Ministry of Education, Science, Culture, Sports, Science, and Technology of Japan (MEXT) (14034230), and JSPS (14380345) to H.S.

REFERENCES

1. **Abdelkhalek, H. B., A. Beckers, K. Schuster-Gossler, M. N. Pavlova, H. Burkhardt, H. Lickert, J. Rossant, R. Reinhardt, L. C. Schalkwyk, I. Muller, B. G. Herrmann, M. Ceolin, R. Rivera-Pomar, and A. Gossler.** 2004. The mouse homeobox gene Not is required for caudal notochord development and affected by the truncate mutation. Genes Dev. **18:**1725–1736.
2. **Anbanandam, A., D. C. Albarado, C. T. Nguyen, G. Halder, X. Gao, and S. Veeraraghavan.** 2006. Insights into transcription enhancer factor 1 (TEF-1) activity from the solution structure of the TEA domain. Proc. Natl. Acad. Sci. USA **103:**17225–17230.
3. **Andrianopoulos, A., and W. E. Timberlake.** 1994. The *Aspergillus nidulans abaA* gene encodes a transcriptional activator that acts as a genetic switch to control development. Mol. Cell. Biol. **14:**2503–2515.
4. **Ang, S. L., and J. Rossant.** 1994. HNF-3 β is essential for node and notochord formation in mouse development. Cell **78:**561–574.
5. **Burke, A. C., C. E. Nelson, B. A. Morgan, and C. Tabin.** 1995. Hox genes and the evolution of vertebrate axial morphology. Development **121:**333–346.
6. **Candia, A. F., J. Hu, J. Crosby, P. A. Lalley, D. Noden, J. H. Nadeau, and C. V. Wright.** 1992. Mox-1 and Mox-2 define a novel homeobox gene subfamily and are differentially expressed during early mesodermal patterning in mouse embryos. Development **116:**1123–1136.
7. **Carninci, P., T. Kasukawa, S. Katayama, J. Gough, M. C. Frith, N. Maeda,**

R. Oyama, T. Ravasi, B. Lenhard, C. Wells, R. Kodzius, K. Shimokawa, V. B. Bajic, S. E. Brenner, S. Batalov, A. R. Forrest, M. Zavolan, M. J. Davis, L. G. Wilming, V. Aidinis, J. E. Allen, A. Ambesi-Impiombato, R. Apweiler, R. N. Aturaliya, T. L. Bailey, M. Bansal, L. Baxter, K. W. Beisel, T. Bersano, H. Bono, A. M. Chalk, K. P. Chiu, V. Choudhary, A. Christoffels, D. R. Clutterbuck, M. L. Crowe, E. Dalla, B. P. Dalrymple, B. de Bono, G. Della Gatta, D. di Bernardo, T. Down, P. Engstrom, M. Fagiolini, G. Faulkner, C. F. Fletcher, T. Fukushima, M. Furuno, S. Futaki, M. Gariboldi, P. Georgii-Hemming, T. R. Gingeras, T. Gojobori, R. E. Green, S. Gustincich, M. Harbers, Y. Hayashi, T. K. Hensch, N. Hirokawa, D. Hill, L. Huminiecki, M. Iacono, K. Ikeo, A. Iwama, T. Ishikawa, M. Jakt, A. Kanapin, M. Katoh, Y. Kawasawa, J. Kelso, H. Kitamura, H. Kitano, G. Kollias, S. P. Krishnan, A. Kruger, S. K. Kummerfeld, I. V. Kurochkin, L. F. Lareau, D. Lazarevic, L. Lipovich, J. Liu, S. Liuni, S. McWilliam, M. Madan Babu, M. Madera, L. Marchionni, H. Matsuda, S. Matsuzawa, H. Miki, F. Mignone, S. Miyake, K. Morris, S. Mottagui-Tabar, N. Mulder, N. Nakano, H. Nakauchi, P. Ng, R. Nilsson, S. Nishiguchi, S. Nishikawa, et al. 2005. The transcriptional landscape of the mammalian genome. Science **309:**1559–1563.

8. **Chapman, D. L., I. Agulnik, S. Hancock, L. M. Silver, and V. E. Papaioannou.** 1996. Tbx6, a mouse T-Box gene implicated in paraxial mesoderm formation at gastrulation. Dev. Biol. **180:**534–542.
9. **Chen, H. H., T. Maeda, S. J. Mullett, and A. F. Stewart.** 2004. Transcription cofactor Vgl-2 is required for skeletal muscle differentiation. Genesis **39:** 273–279.
10. **Chen, H. H., S. J. Mullett, and A. F. Stewart.** 2004. Vgl-4, a novel member of the vestigial-like family of transcription cofactors, regulates alpha1-adrenergic activation of gene expression in cardiac myocytes. J. Biol. Chem. **279:** 30800–30806.
11. **Chen, Z., G. A. Friedrich, and P. Soriano.** 1994. Transcriptional enhancer factor 1 disruption by a retroviral gene trap leads to heart defects and embryonic lethality in mice. Genes Dev. **8:**2293–2301.
12. **Davidson, I., J. H. Xiao, R. Rosales, A. Staub, and P. Chambon.** 1988. The HeLa cell protein TEF-1 binds specifically and cooperatively to two SV40 enhancer motifs of unrelated sequence. Cell **54:**931–942.
13. **Dong, J., G. Feldmann, J. Huang, S. Wu, N. Zhang, S. A. Comerford, M. F. Gayyed, R. A. Anders, A. Maitra, and D. Pan.** 2007. Elucidation of a universal size-control mechanism in *Drosophila* and mammals. Cell **130:**1120–1133.
14. **Downs, K. M., and T. Davies.** 1993. Staging of gastrulating mouse embryos by morphological landmarks in the dissecting microscope. Development **118:**1255–1266.
15. **Dziadek, M., and E. Adamson.** 1978. Localization and synthesis of alphafoetoprotein in post-implantation mouse embryos. J. Embryol. Exp. Morphol. **43:**289–313.
16. **Fossdal, R., F. Jonasson, G. T. Kristjansdottir, A. Kong, H. Stefansson, S. Gosh, J. R. Gulcher, and K. Stefansson.** 2004. A novel TEAD1 mutation is the causative allele in Sveinsson's chorioretinal atrophy (helicoid peripapillary chorioretinal degeneration). Hum. Mol. Genet. **13:**975–981.
17. **Garg, A., A. Srivastava, M. M. Davis, S. L. O'Keefe, L. Chow, and J. B. Bell.** 2007. Antagonizing scalloped with a novel vestigial construct reveals an important role for scalloped in *Drosophila melanogaster* leg, eye and optic lobe development. Genetics **175:**659–669.
18. **Gavrias, V., A. Andrianopoulos, C. J. Gimeno, and W. E. Timberlake.** 1996. *Saccharomyces cerevisiae* TEC1 is required for pseudohyphal growth. Mol. Microbiol. **19:**1255–1263.
19. **Gupta, M., P. Kogut, F. J. Davis, N. S. Belaguli, R. J. Schwartz, and M. P. Gupta.** 2001. Physical interaction between the MADS box of serum response factor and the TEA/ATTS DNA-binding domain of transcription enhancer factor-1. J. Biol. Chem. **276:**10413–10422.
20. **Gupta, M. P., C. S. Amin, M. Gupta, N. Hay, and R. Zak.** 1997. Transcription enhancer factor 1 interacts with a basic helix-loop-helix zipper protein, Max, for positive regulation of cardiac alpha-myosin heavy-chain gene expression. Mol. Cell. Biol. **17:**3924–3936.
21. **Guss, K. A., C. E. Nelson, A. Hudson, M. E. Kraus, and S. B. Carroll.** 2001. Control of a genetic regulatory network by a selector gene. Science **292:** 1164–1167.
22. **Halder, G., P. Polaczyk, M. E. Kraus, A. Hudson, J. Kim, A. Laughon, and S. Carroll.** 1998. The Vestigial and Scalloped proteins act together to directly regulate wing-specific gene expression in *Drosophila*. Genes Dev. **12:**3900–3909.
23. **Herrmann, B. G.** 1991. Expression pattern of the Brachyury gene in whole-mount TWis/TWis mutant embryos. Development **113:**913–917.
24. **Hossain, Z., S. M. Ali, H. L. Ko, J. Xu, C. P. Ng, K. Guo, Z. Qi, S. Ponniah, W. Hong, and W. Hunziker.** 2007. Glomerulocystic kidney disease in mice with a targeted inactivation of Wwtr1. Proc. Natl. Acad. Sci. USA **104:**1631–1636.
25. **Huang, J., S. Wu, J. Barrera, K. Matthews, and D. Pan.** 2005. The Hippo signaling pathway coordinately regulates cell proliferation and apoptosis by inactivating Yorkie, the *Drosophila* Homolog of YAP. Cell **122:**421–434.
26. **Jacquemin, P., J. J. Hwang, J. A. Martial, P. Dolle, and I. Davidson.** 1996. A novel family of developmentally regulated mammalian transcription factors containing the TEA/ATTS DNA binding domain. J. Biol. Chem. **271:**21775–21785.
27. **Jacquemin, P., V. Sapin, E. Alsat, D. Evain-Brion, P. Dolle, and I. Davidson.** 1998. Differential expression of the TEF family of transcription factors in the murine placenta and during differentiation of primary human trophoblasts in vitro. Dev. Dyn. **212:**423–436.
28. **Kanai-Azuma, M., Y. Kanai, J. M. Gad, Y. Tajima, C. Taya, M. Kurohmaru, Y. Sanai, H. Yonekawa, K. Yazaki, P. P. Tam, and Y. Hayashi.** 2002. Depletion of definitive gut endoderm in Sox17-null mutant mice. Development **129:**2367–2379.
29. **Kaneko, K. J., E. B. Cullinan, K. E. Latham, and M. L. DePamphilis.** 1997. Transcription factor mTEAD-2 is selectively expressed at the beginning of zygotic gene expression in the mouse. Development **124:**1963–1973.
30. **Kaneko, K. J., and M. L. DePamphilis.** 1998. Regulation of gene expression at the beginning of mammalian development and the TEAD family of transcription factors. Dev. Genet. **22:**43–55.
31. **Kaneko, K. J., M. J. Kohn, C. Liu, and M. L. DePamphilis.** 2007. Transcription factor TEAD2 is involved in neural tube closure. Genesis **45:**577–587.
32. **Karasseva, N., G. Tsika, J. Ji, A. Zhang, X. Mao, and R. Tsika.** 2003. Transcription enhancer factor 1 binds multiple muscle MEF2 and A/T-rich elements during fast-to-slow skeletal muscle fiber type transitions. Mol. Cell. Biol. **23:**5143–5164.
33. **Kim, J., A. Sebring, J. J. Esch, M. E. Kraus, K. Vorwerk, J. Magee, and S. B. Carroll.** 1996. Integration of positional signals and regulation of wing formation and identity by *Drosophila* vestigial gene. Nature **382:**133–138.
34. **Kitsukawa, T., M. Shimizu, M. Sanbo, T. Hirata, M. Taniguchi, Y. Bekku, T. Yagi, and H. Fujisawa.** 1997. Neuropilin-semaphorin III/D-mediated chemorepulsive signals play a crucial role in peripheral nerve projection in mice. Neuron **19:**995–1005.
35. **Lai, Z. C., X. Wei, T. Shimizu, E. Ramos, M. Rohrbaugh, N. Nikolaidis, L. L. Ho, and Y. Li.** 2005. Control of cell proliferation and apoptosis by mob as tumor suppressor, *mats*. Cell **120:**675–685.
36. **Li, Y., J. Pei, H. Xia, H. Ke, H. Wang, and W. Tao.** 2003. Lats2, a putative tumor suppressor, inhibits G1/S transition. Oncogene **22:**4398–4405.
37. **Maeda, T., D. L. Chapman, and A. F. Stewart.** 2002. Mammalian vestigial-like 2, a cofactor of TEF-1 and MEF2 transcription factors that promotes skeletal muscle differentiation. J. Biol. Chem. **277:**48889–48898.
38. **Mahlapuu, M., M. Ormestad, S. Enerback, and P. Carlsson.** 2001. The forkhead transcription factor Foxf1 is required for differentiation of extra-embryonic and lateral plate mesoderm. Development **128:**155–166.
39. **Mahoney, W. M., Jr., J. H. Hong, M. B. Yaffe, and I. K. Farrance.** 2005. The transcriptional co-activator TAZ interacts differentially with transcriptional enhancer factor-1 (TEF-1) family members. Biochem. J. **388:**217–225.
40. **Matsuo, I., S. Kuratani, C. Kimura, N. Takeda, and S. Aizawa.** 1995. Mouse Otx2 functions in the formation and patterning of rostral head. Genes Dev. **9:**2646–2658.
41. **Milewski, R. C., N. C. Chi, J. Li, C. Brown, M. M. Lu, and J. A. Epstein.** 2004. Identification of minimal enhancer elements sufficient for Pax3 expression in neural crest and implication of Tead2 as a regulator of Pax3. Development **131:**829–837.
42. **Morin-Kensicki, E. M., B. N. Boone, M. Howell, J. R. Stonebraker, J. Teed, J. G. Alb, T. R. Magnuson, W. O'Neal, and S. L. Milgram.** 2006. Defects in yolk sac vasculogenesis, chorioallantoic fusion, and embryonic axis elongation in mice with targeted disruption of Yap65. Mol. Cell. Biol. **26:**77–87.
43. **Murata, T., K. Furushima, M. Hirano, H. Kiyonari, M. Nakamura, Y. Suda, and S. Aizawa.** 2004. *ang* is a novel gene expressed in early neuroectoderm, but its null mutant exhibits no obvious phenotype. Gene Expr. Patterns **5:**171–178.
44. **Nishioka, N., S. Yamamoto, H. Kiyonari, H. Sato, A. Sawada, M. Ota, K. Nakao, and H. Sasaki.** 2007. *Tead4* is required for specification of trophectoderm in pre-implantation mouse embryos. Mech. Dev. doi:10.1016/j.mod.2007.11.002.
45. **Overholtzer, M., J. Zhang, G. A. Smolen, B. Muir, W. Li, D. C. Sgroi, C. X. Deng, J. S. Brugge, and D. A. Haber.** 2006. Transforming properties of YAP, a candidate oncogene on the chromosome 11q22 amplicon. Proc. Natl. Acad. Sci. USA **103:**12405–12410.
46. **Pan, D.** 2007. Hippo signaling in organ size control. Genes Dev. **21:**886–897.
47. **Sasaki, H., and B. L. Hogan.** 1993. Differential expression of multiple fork head related genes during gastrulation and axial pattern formation in the mouse embryo. Development **118:**47–59.
48. **Sasaki, H., and B. L. Hogan.** 1996. Enhancer analysis of the mouse HNF-3β gene: regulatory elements for node/notochord and floor plate are independent and consist of multiple sub-elements. Genes Cells **1:**59–72.
49. **Sawada, A., Y. Nishizaki, H. Sato, Y. Yada, R. Nakayama, S. Yamamoto, N. Nishioka, H. Kondoh, and H. Sasaki.** 2005. Tead proteins activate the Foxa2 enhancer in the node in cooperation with a second factor. Development **132:**4719–4729.
50. **Schweizer, A., S. Rupp, B. N. Taylor, M. Rollinghoff, and K. Schroppel.** 2000. The TEA/ATTS transcription factor CaTec1p regulates hyphal development and virulence in *Candida albicans*. Mol. Microbiol. **38:**435–445.
51. **Sham, M. H., C. Vesque, S. Nonchev, H. Marshall, M. Frain, R. D. Gupta, J. Whiting, D. Wilkinson, P. Charnay, and R. Krumlauf.** 1993. The zinc

finger gene Krox20 regulates HoxB2 (Hox2.8) during hindbrain segmentation. Cell **72:**183–196.
52. **Simeone, A., D. Acampora, M. Gulisano, A. Stornaiuolo, and E. Boncinelli.** 1992. Nested expression domains of four homeobox genes in developing rostral brain. Nature **358:**687–690.
53. **Simmonds, A. J., X. Liu, K. H. Soanes, H. M. Krause, K. D. Irvine, and J. B. Bell.** 1998. Molecular interactions between Vestigial and Scalloped promote wing formation in *Drosophila*. Genes Dev. **12:**3815–3820.
54. **Srivastava, A., A. J. Simmonds, A. Garg, L. Fossheim, S. D. Campbell, and J. B. Bell.** 2004. Molecular and functional analysis of scalloped recessive lethal alleles in *Drosophila melanogaster*. Genetics **166:**1833–1843.
55. **Strano, S., O. Monti, N. Pediconi, A. Baccarini, G. Fontemaggi, E. Lapi, F. Mantovani, A. Damalas, G. Citro, A. Sacchi, G. Del Sal, M. Levrero, and G. Blandino.** 2005. The transcriptional coactivator Yes-associated protein drives p73 gene-target specificity in response to DNA Damage. Mol. Cell **18:**447–459.
56. **Sun, X., E. N. Meyers, M. Lewandoski, and G. R. Martin.** 1999. Targeted disruption of Fgf8 causes failure of cell migration in the gastrulating mouse embryo. Genes Dev. **13:**1834–1846.
57. **Tao, W., S. Zhang, G. S. Turenchalk, R. A. Stewart, M. A. St John, W. Chen, and T. Xu.** 1999. Human homologue of the *Drosophila melanogaster lats* tumour suppressor modulates CDC2 activity. Nat. Genet. **21:**177–181.
58. **Vassilev, A., K. J. Kaneko, H. Shu, Y. Zhao, and M. L. DePamphilis.** 2001. TEAD/TEF transcription factors utilize the activation domain of YAP65, a Src/Yes-associated protein localized in the cytoplasm. Genes Dev. **15:**1229–1241.
59. **Vaudin, P., R. Delanoue, I. Davidson, J. Silber, and A. Zider.** 1999. TONDU (TDU), a novel human protein related to the product of vestigial (vg) gene of *Drosophila melanogaster* interacts with vertebrate TEF factors and substitutes for Vg function in wing formation. Development **126:**4807–4816.
60. **Weinstein, D. C., A. Ruiz i Altaba, W. S. Chen, P. Hoodless, V. R. Prezioso, T. M. Jessell, and J. E. Darnell, Jr.** 1994. The winged-helix transcription factor HNF-3 β is required for notochord development in the mouse embryo. Cell **78:**575–588.
61. **Wilkinson, D. G.** 1992. Whole mount in situ hybridization of vertebrate embryos., p. 75–84. *In* D. G. Wilkinson (ed.), In situ hybridization: a practical approach. IRL Press, Oxford, United Kingdom.
62. **Wilkinson, D. G., S. Bhatt, M. Cook, E. Boncinelli, and R. Krumlauf.** 1989. Segmental expression of Hox-2 homeobox-containing genes in the developing mouse hindbrain. Nature **341:**405–409.
63. **Wu, J., A. Duggan, and M. Chalfie.** 2001. Inhibition of touch cell fate by egl-44 and egl-46 in *C. elegans*. Genes Dev. **15:**789–802.
64. **Wu, S., J. Huang, J. Dong, and D. Pan.** 2003. hippo encodes a Ste-20 family protein kinase that restricts cell proliferation and promotes apoptosis in conjunction with salvador and warts. Cell **114:**445–456.
65. **Xiao, J. H., I. Davidson, H. Matthes, J. M. Garnier, and P. Chambon.** 1991. Cloning, expression, and transcriptional properties of the human enhancer factor TEF-1. Cell **65:**551–568.
66. **Yagi, R., L. F. Chen, K. Shigesada, Y. Murakami, and Y. Ito.** 1999. A WW domain-containing yes-associated protein (YAP) is a novel transcriptional co-activator. EMBO J. **18:**2551–2562.
67. **Yagi, R., M. J. Kohn, I. Karavanova, K. J. Kaneko, D. Vullhorst, M. L. Depamphilis, and A. Buonanno.** 2007. Transcription factor TEAD4 specifies the trophectoderm lineage at the beginning of mammalian development. Development **134:**3827–3836.
68. **Yagi, T., T. Tokunaga, Y. Furuta, S. Nada, M. Yoshida, T. Tsukada, Y. Saga, N. Takeda, Y. Ikawa, and S. Aizawa.** 1993. A novel ES cell line, TT2, with high germline-differentiating potency. Anal. Biochem. **214:**70–76.
69. **Yamaguchi, T. P., S. Takada, Y. Yoshikawa, N. Wu, and A. P. McMahon.** 1999. T (Brachyury) is a direct target of Wnt3a during paraxial mesoderm specification. Genes Dev. **13:**3185–3190.
70. **Yockey, C. E., G. Smith, S. Izumo, and N. Shimizu.** 1996. cDNA cloning and characterization of murine transcriptional enhancer factor-1-related protein 1, a transcription factor that binds to the M-CAT motif. J. Biol. Chem. **271:**3727–3736.
71. **Yu, H., R. F. Pretot, T. R. Burglin, and P. W. Sternberg.** 2003. Distinct roles of transcription factors EGL-46 and DAF-19 in specifying the functionality of a polycystin-expressing sensory neuron necessary for *C. elegans* male vulva location behavior. Development **130:**5217–5227.
72. **Zender, L., M. S. Spector, W. Xue, P. Flemming, C. Cordon-Cardo, J. Silke, S. T. Fan, J. M. Luk, M. Wigler, G. J. Hannon, D. Mu, R. Lucito, S. Powers, and S. W. Lowe.** 2006. Identification and validation of oncogenes in liver cancer using an integrative oncogenomic approach. Cell **125:**1253–1267.